

Graph Edits for Counterfactual Explanations: A Unified GNN Approach

Nikolaos Chaidos*, Angeliki Dimitriou*, Maria Lymperaioi, Giorgos Stamou

Artificial Intelligence and Learning Systems Laboratory
School of Electrical and Computer Engineering
National Technical University of Athens

Abstract

Counterfactuals have been established as a popular explainability technique which leverages a set of minimal edits to alter the prediction of a classifier. When considering conceptual counterfactuals, the edits requested should correspond to salient concepts present in the input data. At the same time, conceptual distances are defined by knowledge graphs, ensuring the optimality of conceptual edits. In this work, we extend previous endeavors on conceptual counterfactuals by introducing *graph edits as counterfactual explanations*: should we represent input data as graphs, which is the shortest graph edit path that results in an alternative classification label as provided by a black-box classifier?

Introduction

In the era of large and complex neural models, ensuring trust between them and human users becomes a critical issue. Explainability literature suggests a variety of methods to probe neural networks behaviors, either requiring access to their inner workings (Goyal et al. 2019; Vandenhende et al. 2022) or not (Filandrianos et al. 2022; Dervakos et al. 2023). There is also lots of discussion regarding the nature of the features involved in a human-understandable explanation; for example, low-level features such as pixel-related characteristics (brightness, contrast) may be unable to provide a meaningful explanation to the end user, despite being informative for a neural model (Rudin 2019). This observation is applicable in the counterfactual explanation scenario, suggesting that semantics are fundamentally essential to meaningful counterfactual explanations (Browne and Swift 2020). In the meanwhile, both high-level semantics as well as low-level features can be expressed in the same mathematical format (e.g. numerical vectors), allowing the transition to semantically rich explanation systems (Dervakos et al. 2023). In the interest of explaining visual classification systems, and with respect to recent related literature (Goyal et al. 2019; Akula, Wang, and Zhu 2020; Vandenhende et al. 2022; Filandrianos et al. 2022; Dervakos et al. 2023), we base our current work on *conceptual counterfactual explanations*.

With regard to the model accessibility an explainability system can have, most related counterfactual explana-

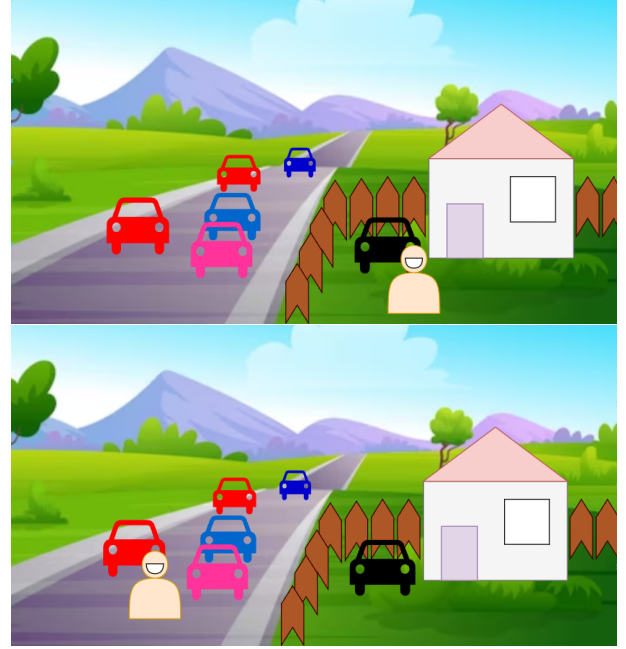


Figure 1: A safe situation of a person in front of a parked car (top) contrary to a non-safe situation of a person in front of moving cars on the highway (bottom).

tion methods belong to the white-box category (Goyal et al. 2019; Akula, Wang, and Zhu 2020; Vandenhende et al. 2022), offering insights tailored to the model under investigation. However, in the emergence of powerful, yet proprietary models, such as ChatGPT (OpenAI 2023a) and GPT-4 (OpenAI 2023b) which are currently accessible only through APIs, black-box explanations resurface as more viable and universal solutions, able to approach a model by appropriately scrutinizing their outputs. Under these constraints, we propose a *black-box conceptual counterfactual framework*, following Filandrianos et al. (2022); Dervakos et al. (2023).

Specifically, the explanation framework proposed in Filandrianos et al. (2022); Dervakos et al. (2023) harnesses the well-defined semantic knowledge existing in knowledge graphs, therefore allowing a deterministic viewpoint of conceptual distances: concepts extracted from images or other

*These authors contributed equally.

modalities can be mapped on the WordNet hierarchy (Miller 1995), which provides a sense of distance based on hypernym/hyponym relationships. We step upon this approach to frame our *knowledge-based counterfactual explanations*.

Nonetheless, explanations derived from Filandrianos et al. (2022); Dervakos et al. (2023) in fact lack a proper interpretation of relationships between concepts. Even the indirect incorporation of roles via ‘role roll-up into concepts’ (Dervakos et al. 2023) may result in erroneous explanations in certain cases: when multiple objects of the same class appear in an image, there can be no distinction between them, therefore the connection with roles and other concepts remains rather uncertain. This approach can be limiting in real world scenarios when associations between concepts via roles may result in different interpretations of situations depicted on images. Let’s consider a self-driving car scenario where a corresponding AI system has to provide an explanation of whether a given scene should be considered as safe or not. Figure 1 depicts such a scenario, where the relationship between the person, the car and the highway is critical. If we derive explanations using Dervakos et al. (2023) we cannot tell if the person stands in front of the moving cars on the highway or in front of the car parked in the garden, therefore we cannot explain a safe/not safe classification.

To overcome this limitation, we propose the utilization of scene graphs in place of role roll-up. Specifically, scene graphs contain nodes and edges representing concepts and roles respectively, while pairing concepts via roles forms triples, allowing a high-level description of a complex image (Chang et al. 2023). In this case, the placement of the person of Figure 1 with respect of the cars and the motorway becomes evident; intuitively, a conceptual counterfactual explanation derived from a scene graph-based explanation algorithm will return those triples that distinguish between safe/not safe situations. Therefore, a natural extension of the techniques of Filandrianos et al. (2022); Dervakos et al. (2023) suggests the optimal matching of scene graphs (i.e. find the most similar scene graph to another scene graph) in place of the optimal matching of sets of image concepts.

Despite being promising in terms of more accurate explanations, graph matching is a computationally hard problem. A measure of similarity between graphs can be estimated using *Graph Edit Distance (GED)* (Sanfeliu and Fu 1983), referring to the minimum cost set of edits needed to transform a graph to another graph. Retrieval of the most similar candidate graph G_c to a reference graph G_r requires finding the minimum GED between the reference G_r and all the candidates. Especially in the case of counterfactual retrieval, the minimum GED candidate G_c should also belong to a different class B compared to the reference graph class A .

In order to overcome the computational complexity of GED calculation, we employ Graph Machine Learning algorithms, such as Graph Kernels, Graph Autoencoders (GAEs) and Graph Neural Networks (GNNs). Such approaches are proven to be lightweight and significantly faster than the deterministic GED calculation, even when optimizations (Jonker and Volgenant 1987) are employed.

The outline of our approach is presented in Figure 2. Overall, this work contributes to the following:

- We propose a framework of *graph-based conceptual counterfactual explanations* overcoming significant limitations of prior work on conceptual counterfactuals.
- We demonstrate the capabilities of unsupervised (GAEs) vs supervised (GNNs) Graph Machine Learning algorithms towards counterfactual explanations.
- We prove quantitatively and qualitatively that both unsupervised and supervised approaches are able to provide meaningful and accurate counterfactual explanations.

Related work

Counterfactual Explanations have been established as an effective explanation method (Wachter, Mittelstadt, and Russell 2018) should certain requirements, such as actionability and feasibility be met (Poyiadzi et al. 2020). These principles are transferred in the field of counterfactual visual explanations, which aim to explain the behaviors of image classifiers. Most of these approaches leverage pixel-level edits, denoting regions that should be minimally changed (Hendricks et al. 2018; Goyal et al. 2019; Vandenhende et al. 2022) and often proceed to actually generate the targeted region by leveraging generative models (Chang et al. 2019; Zhao, Oyama, and Kurihara 2020; Augustin et al. 2022; Farid et al. 2023).

Since semantics are inherently tied to human-interpretable counterfactuals (Browne and Swift 2020), a diverging line of work suggests moving towards conceptual rather than pixel-level counterfactuals. The notion of explainable concepts was presented in Akula, Wang, and Zhu (2020), where fault-lines are utilized to drive concept edits. Abid, Yuksekogunul, and Zou (2022) produce conceptual counterfactuals to meaningfully explain model misclassifications. However, these approaches require some degree of access to the internals of the classifier. Minimal concept edits in a black-box fashion were proposed in Filandrianos et al. (2022), paving the way for knowledge-based model-agnostic visual counterfactual explanations. Some limitations were resolved in the subsequent work of Dervakos et al. (2023), suggesting an indirect incorporation of roles into concepts, while underlining the importance of correctly selecting datasets and concept extraction methods to obtain proper explanations. The same idea is modified to explain hallucinations of image generation models rather than classifiers (Lymperaoui et al. 2023), highlighting the significance of universal black-box explainers.

Method

Background

The core of the current work revolves around the fundamental question of “What is the minimal *semantic* change that has to occur in order for an image i to be classified as B instead of A ?”. Each image i in our dataset I is represented by a scene graph G_i , comprising nodes and edges that contain *semantics* s , ultimately constituting an *explanation dataset* $\{i, G_i\}$, $i \in I$ as in Filandrianos et al. (2022).

Considering a reference image i_r with corresponding scene graph G_{i_r} , and candidates $G_{i_c}, c \in C = \{I \setminus i_r\}$,

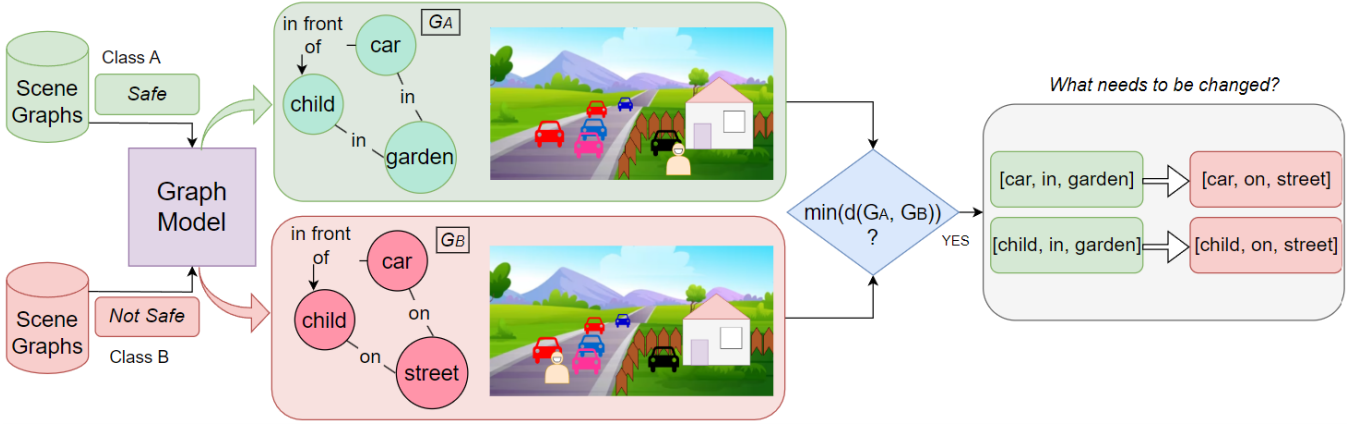


Figure 2: Outline of our approach: Given scene graphs of classes $A \neq B$, a graph model embeds them in a low-dimensional space, allowing the retrieval of the closest G_A, G_B from which we extract counterfactual edits.

GED between G_{i_r} and a random candidate is expressed as:

$$GED(G_{i_r}, G_{i_c}) = \min_{(e_1, \dots, e_n) \in P(G_{i_r}, G_{i_c})} \sum_{i=1}^n c(e_i) \quad (1)$$

where $c(e)$ denotes the cost of a graph edit operation e among n possible valid edits, and $P(G_{i_r}, G_{i_c})$ corresponds to the set of graph paths needed to transform G_{i_r} to G_{i_c} .

Graph edits $e \in \{R, D, I\}$ can be either of the following:

- **Replacement (R)** of semantics of G_{i_r} with semantics of G_{i_c}
- **Deletion (D)** of semantics of G_{i_r}
- **Insertion (I)** of semantics to G_{i_r}

The semantic distances guiding the choice of e are imposed from a selected knowledge source, in our case being WordNet (Miller 1995), ensuring that a minimal path between G_{i_r} and G_{i_c} semantics exists and can be deterministically found. In practical terms, WordNet permits meaningful and actionable transitions by enforcing semantically related edits such as replacing e.g. 'pedestrian' \rightarrow 'human', while penalizing irrelevant replacements with high distances (e.g. 'pedestrian' \rightarrow 'sea'), so that they are unlikely to appear in the derived edit path. At the same time, minimal changes are essentially one of the desiderata of counterfactual explanations, where small input perturbations result in significant changes in the outcome (in our case being the predicted classification label). WordNet can be easily linked to various machine learning datasets via object and relationship *synsets*, i.e. sets of synonyms expressing the same concept.

Since GED calculation of Eq. 1 for a pair of graphs is an NP-hard problem, optimization techniques are employed for acceleration; we use the Volgenant-Jonker (VJ) (Jonker and Volgenant 1987) assignment algorithm to drop the complexity to $O(v^3)$, where v is the number of vertices on the scene graph, rendering this approximation inefficient for larger graphs. In order to retrieve the counterfactual candidate $G_{i_{cc}}$ we repeat the optimized VJ GED calculation for each candidate $c \in C$ imposing that the selected closest G_{i_c} belongs to

class B , while $G_{i_r} \in A \neq B$:

$$G_{i_{cc}} = \min_{c \in C} (GED(G_{i_r}, G_{i_c})), G_{i_r} \in A, G_{i_c} \in B \neq A \quad (2)$$

The importance of Graph Machine Learning

Considering a dataset with N graphs, calculating the counterfactual $G_{i_{cc}}$ for every G_{i_r} requires $O(N^2)$ GED operations, resulting in a prohibitive calculation time, despite using optimizations. In order to accelerate this process, we leverage Graph Machine Learning algorithms to circumvent the exhaustive calculation of N^2 GEDs, accepting an unavoidable performance sacrifice.

Graph Kernels is our first step towards testing graph matching (Kondor 2002). Kernels in Machine Learning are responsible for mapping the given data in high-dimensional spaces, revealing complex patterns that cannot be observed in the original dimensionality of the input data, therefore allowing the application of linear algorithms to solve non-linear problems. Graph kernels quantify the degree of similarity between subgraphs in polynomial time by employing kernel functions, thus contributing to the overall structural similarity between two given graphs. In our experiments, we will compare different graph kernel approaches.

Graph Neural Networks (GNNs) Moving on to neural implementations, there are both supervised and unsupervised techniques able to provide efficient GED approximations. In the supervised setting, GNN architectures such as Graph Convolution Network (GCN) (Kipf and Welling 2016a), Graph Attention Network (GAT) (Veličković et al. 2017), and Graph Isomorphism Network (GIN) (Xu et al. 2018) can be incorporated in a Siamese Network to learn similarity on input instances (Li et al. 2019), demonstrating state-of-the-art results even when trained on a smaller subset of N^2/j labeled graph pairs (N is the number of graphs in the complete dataset, j a small, positive integer). During training, these GNN variants learn the relationships between counterfactual graph pairs utilizing ground truth samples as calculated from Eq. 2. Embedding representations

on new graphs are extracted using the trained GNNs, translating graph similarity cues to distances in the embedding space, therefore allowing retrieval of counterfactual graphs G_{ic} for each given G_{ir} .

Graph Autoencoders (GAEs) By eliminating the need for labeled samples, unsupervised techniques such as GAEs (Kipf and Welling 2016b) arise as faster and more versatile solutions, even though their metric performance often ranks lower than GNNs. GAEs comprise of an encoder-decoder structure, with the encoder being tasked to produce embedding representations; these representations are useful for retrieval tasks, since similarity in the embedding space corresponds to actual graph similarity. Thus, the need of GED calculations within the training process is completely avoided, dropping the computational complexity to $O(N)$ in comparison to the $O(N^2)$ operations required in the supervised case (N is the number of graphs). The encoder and decoder modules are constructed using any of the aforementioned GNN variants (same GNN modules for the encoder and the decoder when applicable).

In all cases, we retain the NP-hard GED scores as ground truth for comparison, so that we evaluate the performance of different graph algorithms on the ground-truth rank.

Graph data and connection with knowledge

In all our experiments, we select Visual Genome (VG) (Krishna et al. 2017) as the experimental dataset, due to its abundance in real-life scenes accompanied by manually annotated scene graphs. In addition, VG offers an effortless connection with WordNet, since synset annotations of objects and roles are also provided by annotators. This connection was implemented via the usage of NLTK (Bird, Klein, and Loper 2009) python package API¹; the same package offers the simple calculation of path similarity scores between two WordNet synsets, providing a number in the $[0, 1]$ range, which denotes the proximity of the synsets within the hierarchy. We repeat the path similarity calculation for all possible node pairs present in selected VG graph pairs G_{ir} , G_{ic} . This way, the replacement (R) cost is defined, by feeding the $1 - \text{path_similarity}$ value to the ground truth GED (Eq. 1). In a similar way, deletion (D) and insertion (I) scores are calculated by finding the shortest path between each G_{ir} node and the root concept of WordNet (entity.n.01).

Dataset splits Since graph edges are important in our proposed method, we regard two dataset splits for training based on scene graph density: the first one, called VG-DENSE includes graphs with many interconnections and fewer isolated nodes, while we also set an upper bound to the number of graph vertices. The second one called VG-RANDOM does not impose any restrictions on scene graph size and density. Both splits contain $N=500$ scene graphs, and we attempt training using varying numbers of scene graph pairs.

Since VG does not contain ground truth labels for scenes we assign labels using a pre-trained PLACES-360 classifier (Zhou et al. 2017). Counterfactual images may belong to any

class defined from PLACES-360, as long as the *query* and the *target* classes differ.

Experiments

Model	NDCG			Precision (P)		
	@4	@2	@1	@4	@2	@1
VG-DENSE						
WL kernel	0.219	0.219	0.224	0.164	0.125	0.076
SP kernel	0.201	0.205	0.205	0.154	0.145	0.122
RW kernel	0.002	0.002	0.0	0.001	0.0	0.0
NH kernel	0.115	0.116	0.107	0.088	0.073	0.05
GS kernel	0.029	0.026	0.026	0.022	0.007	0.008
Superv. GAT	0.400	0.39	0.375	0.312	0.25	0.164
Superv. GIN	0.346	0.346	0.338	0.252	0.192	0.158
Superv. GCN	0.457	0.456	0.445	0.358	0.292	0.248
GAE GAT	0.103	0.11	0.109	0.075	0.075	0.048
GAE GIN	0.116	0.121	0.119	0.082	0.078	0.052
GAE GCN	0.091	0.096	0.094	0.071	0.06	0.052
VGAE GAT	0.189	0.193	0.185	0.139	0.12	0.082
VGAE GIN	0.190	0.194	0.192	0.141	0.119	0.09
VGAE GCN	0.167	0.169	0.161	0.122	0.101	0.066
GFA GAT	0.178	0.184	0.178	0.122	0.109	0.086
GFA GIN	0.191	0.195	0.195	0.14	0.122	0.096
GFA GCN	0.163	0.165	0.158	0.12	0.104	0.068
ARVGA GAT	0.181	0.186	0.18	0.132	0.114	0.084
ARVGA GIN	0.192	0.2	0.199	0.135	0.124	0.106
ARVGA GCN	0.170	0.174	0.17	0.122	0.106	0.076
VG-RANDOM						
WL kernel	0.189	0.192	0.213	0.13	0.108	0.096
SP kernel	0.115	0.118	0.123	0.079	0.068	0.064
RW kernel	0.012	0.01	0.009	0.007	0.0	0.0
NH kernel	0.19	0.196	0.212	0.135	0.116	0.092
GS kernel	0.007	0.006	0.003	0.05	0.0	0.0
Superv. GAT	0.394	0.396	0.395	0.294	0.245	0.176
Superv. GIN	0.333	0.337	0.34	0.245	0.205	0.144
Superv. GCN	0.400	0.397	0.401	0.295	0.246	0.2
GAE GAT	0.132	0.14	0.151	0.092	0.085	0.07
GAE GIN	0.117	0.127	0.133	0.08	0.076	0.07
GAE GCN	0.12	0.13	0.141	0.079	0.078	0.066
VGAE GAT	0.158	0.17	0.182	0.103	0.1	0.09
VGAE GIN	0.16	0.173	0.186	0.11	0.101	0.088
VGAE GCN	0.156	0.167	0.18	0.101	0.089	0.088
GFA GAT	0.157	0.169	0.185	0.107	0.094	0.076
GFA GIN	0.158	0.17	0.183	0.11	0.093	0.082
GFA GCN	0.157	0.168	0.184	0.106	0.095	0.082
ARVGA GAT	0.167	0.18	0.193	0.111	0.103	0.092
ARVGA GIN	0.17	0.181	0.194	0.116	0.099	0.084
ARVGA GCN	0.166	0.179	0.193	0.113	0.097	0.094

Table 1: Counterfactual retrieval results using Supervised and Unsupervised GNN architectures. Underlined cells correspond to best results per graph model choice (kernel, supervised, unsupervised). **Bold** denotes the best results overall per dataset split.

¹<https://www.nltk.org/howto/wordnet.html>

Model	NDCG (binary)			Precision (P) (binary)		
	@4	@2	@1	@4	@2	@1
VG-DENSE						
WL kernel	0.287	0.198	0.138	0.186	0.128	0.076
SP kernel	<u>0.334</u>	<u>0.251</u>	<u>0.194</u>	<u>0.232</u>	<u>0.174</u>	<u>0.122</u>
RW kernel	0.0	0.0	0.0	0.0	0.0	0.0
NH kernel	0.282	0.192	0.131	0.124	0.086	0.05
GS kernel	0.259	0.166	0.103	0.018	0.008	0.008
Superv. GAT	0.342	0.26	0.204	0.422	0.288	0.164
Superv. GIN	0.339	0.256	0.2	0.344	0.242	0.158
Superv. GCN	0.407	0.333	0.283	0.492	0.37	0.248
GAE GAT	0.281	0.191	0.13	0.108	0.078	0.048
GAE GIN	0.281	0.191	0.13	0.132	0.098	0.052
GAE GCN	0.287	0.197	0.137	0.102	0.078	0.052
VGAE GAT	0.298	0.21	0.15	0.196	0.138	0.082
VGAE GIN	0.304	0.216	0.157	0.202	0.146	0.09
VGAE GCN	0.287	0.198	0.137	0.174	0.118	0.066
GFA GAT	0.302	0.214	0.155	0.182	0.14	0.086
GFA GIN	0.309	0.223	0.164	0.21	0.148	0.096
GFA GCN	0.163	0.165	0.158	<u>0.289</u>	<u>0.2</u>	<u>0.139</u>
ARVGA GAT	0.3	0.213	0.153	0.188	0.14	0.084
ARVGA GIN	<u>0.317</u>	<u>0.232</u>	<u>0.174</u>	0.218	0.164	0.106
ARVGA GCN	<u>0.295</u>	<u>0.207</u>	<u>0.146</u>	0.184	0.138	0.076
VG-RANDOM						
WL kernel	<u>0.306</u>	<u>0.219</u>	<u>0.16</u>	0.166	<u>0.124</u>	<u>0.096</u>
SP kernel	0.292	0.204	0.144	0.11	0.09	0.064
RW kernel	0.0	0.0	0.0	0.0	0.0	0.0
NH kernel	0.303	0.216	0.157	<u>0.168</u>	0.116	0.092
GS kernel	0.0	0.0	0.0	0.002	0.0	0.0
Superv. GAT	0.35	0.268	0.213	0.382	0.294	0.176
Superv. GIN	<u>0.327</u>	<u>0.243</u>	<u>0.186</u>	0.308	0.228	0.144
Superv. GCN	0.369	0.29	0.236	0.424	0.3	0.2
GAE GAT	0.294	0.205	0.146	0.132	0.104	0.07
GAE GIN	0.297	0.209	0.15	0.114	0.096	0.07
GAE GCN	0.291	0.203	0.143	0.114	0.1	0.066
VGAE GAT	0.305	0.218	0.159	0.16	0.122	0.09
VGAE GIN	0.304	0.217	0.158	0.152	0.118	0.088
VGAE GCN	0.303	0.216	0.157	<u>0.156</u>	0.122	0.088
GFA GAT	0.292	0.203	0.143	0.142	0.108	0.076
GFA GIN	0.298	0.211	0.151	0.142	0.11	0.082
GFA GCN	0.297	0.209	0.149	0.14	0.112	0.082
ARVGA GAT	0.305	0.218	0.159	<u>0.156</u>	<u>0.13</u>	0.092
ARVGA GIN	0.298	0.21	0.15	0.152	0.118	0.084
ARVGA GCN	<u>0.306</u>	<u>0.22</u>	<u>0.161</u>	0.154	<u>0.13</u>	<u>0.094</u>

Table 2: Counterfactual retrieval results using Supervised and Unsupervised GNN architectures for *binary* ranking metrics. Underlined cells correspond to best results per graph model choice (kernel, supervised, unsupervised). **Bold** denotes the best results overall per dataset split.

Experimental setup

In this work, the implemented graph kernels are the following: Shortest Path (SP) Kernel (Borgwardt and Krieger 2005) (selecting "Auto" as the underlying algorithm searching for the shortest path), Weisfeiler-Lehman (WL) Kernel (Shervashidze et al. 2011), Neighborhood Hash (NH) Ker-

nel (Hido and Kashima 2009), Random Walk (RW) Kernel (Gärtner, Flach, and Wrobel 2003) and Graphlet Sampling (GS) Kernel (Pržulj 2007). Graph kernel modules were implemented using the GraKel library (Siglidis et al. 2020).

The supervised GNN modules used in our work are the aforementioned single-layer GCN, GAT and GIN, trained for 50 epochs, selecting batch size 32 and Adam as the optimizer without weight decay.

As for GAEs, we implement the vanilla GAE, as well as the Variational GAE (VGAE) (Kipf and Welling 2016b), which are both based on the generic auto-encoder structure, but differing in terms of the implemented loss function. Moreover, we experiment with the Adversarially Regularized Variational Graph Autoencoder (ARVGA) (Pan et al. 2019), which employs some basic concepts from the Generative Adversarial Networks (Goodfellow et al. 2014), in order to further boost the regularization of the latent embeddings produced by VGAE. Finally, we also evaluate a variation of the Graph Feature Autoencoder (GFA) proposed in (Hasibi and Michoel 2020), where we utilize the Feature Decoder (whose goal is to predict the feature matrix X), alongside the original VGAE Inner-Product Decoder (whose goal is to predict the adjacency matrix A). For all these GAE variants, we test single-layer GCN, GAT and GIN architectures in the encoder (and the decoder for GFA). AdamW (Loshchilov and Hutter 2019) was selected as the optimizer, maintaining the default parameters ($\beta_1 = 0.9$, $\beta_2 = 0.999$, $\text{weight_decay} = 0.01$), while the initial learning rate is set to 0.001. We train for 20 epochs with a batch size of 32.

GNNs and GAEs were implemented using PyTorch Geometric (Fey and Lenssen 2019). In all cases, cosine similarity was used as a measure for embedding similarity. For each scene graph from the dataset acting as the *query*, we retrieve the closest k graphs of different PLACES-360 label, and we evaluate whether the counterfactual graph according to ground truth GED was found in this rank of k items.

Evaluation Information retrieval metrics (Manning, Raghavan, and Schütze 2008) are employed for evaluation, specifically Precision ($P@k$) and Normalized Discounted Cumulative Gain ($NDCG@k$). $P@k$ returns the percentage of the relevant items, when considering the first k items in the rank. $NDCG@k$ compares the rank returned from an algorithm compared to the ideal ground truth rank (as given from the ground truth GED of Eq. 1), considering the first k items retrieved. All the top- k GED-retrieved items are considered to be relevant and equally weighted.

We propose a "binary" variant of these metrics, which only regards the top-1 GED item as relevant, and all the rest as irrelevant. This arrangement is important for counterfactual calculation, because the only truly correct retrieved instance is the minimum cost one belonging to a different class. Our evaluation includes ranks for $k=1, 2, 4$, emphasizing proximity to the top-1 result for the same rationale.

Quantitative Results

In Tables 1, 2, we present our quantitative results regarding counterfactual retrieval using a variety of graph models: graph kernels, supervised GNNs and unsupervised graph au-

toencoders. For both dataset subsets, all supervised models were trained using 70K scene graph pairs extracted from $N=500$ graphs, while all unsupervised models were trained on the same 500 graphs (without pairing them).

Kernels demonstrate some interesting patterns in results, with some kernels scoring close to unsupervised autoencoders: in VG-DENSE, SP (binary metrics, see Tab. 2) and WL (typical ranking metrics, Tab. 1) score higher than the rest, while the same holds for WL and NH in VG-RANDOM. On the other hand, SP metrics in VG-RANDOM and NH metrics in VG-DENSE are not satisfactory, demonstrating that the number of edges plays a definitive role in their performance. In fact, in the case of the sparser VG-RANDOM subset, kernels like SP are incapable of performing well due to their emphasis on structure and connectivity, whereas NH, being the closest one in nature to GNNs, still holds its ground. On the contrary, some other kernel architectures are completely incapable of retrieving counterfactual graphs, such as RW kernel in both dataset splits, which scores 0 in all metrics. GS kernel also tends to consistently score very low. These results can be interpreted based on the fundamentals of these architectures, which search for structural graph properties such as prototype patterns (graphlets), while being based on shortest path and random walk algorithms; these properties ignore *semantics* of scene graphs.

Quite unsurprisingly, supervised GNN models demonstrate better performance in all ranking metrics, with the most successful variant being GCN. These results are somehow expected, since supervised GNNs have been optimized on the ground truth GED, learning patterns that instruct similarities and dissimilarities of graphs. Unsupervised autoencoders present more variability in results; in the VG-DENSE split, ARVGA GIN achieves best scores in most metrics. In the VG-RANDOM split, ARVGA GIN remains the top scorer for non-binary metrics, but shares the first position with the other variants for binary ones. In both VG-DENSE and VG-RANDOM splits, no GAE or GFA model is able to achieve a competitive ranking score, emphasizing the impactful contribution of Adversarial Regularization.

Regarding the non-monotonic behavior of NDCG, we observe that the score does not necessarily decrease as we include more retrieved objects. This phenomenon is commonplace in the context of Information Retrieval tasks, and it reflects the system’s capability to compensate for potential inaccuracies at the top rank by retrieving a well-ordered and relevant set of objects within a broader scope. For example, a model could score better on NDCG@4 than NDCG@1, in the case where the top-retrieved object is incorrect, yet the subsequent objects in the ranking prove to be highly relevant to the ground truth rank.

By comparing ranking metrics across the two dataset splits, we can easily observe that best results overall were achieved in the DENSE split. This is an expected behavior, since GNNs require interconnections for message passing procedures, i.e. to exchange and aggregate information from their neighbors.

Performance vs dataset size Even though unsupervised autoencoder results stay behind supervised ones, there is a significant difference in terms of ground truth data needed. Specifically, supervised GNNs were trained on 70K pairs, which equals to $\sim N^2/2$ pairs, maintaining a quadratical relationship with the input data size. Apart from that, the construction of these $O(N^2)$ pairs requires the calculation of the already computationally expensive ground truth GED of Eq. 1. On the other hand, unsupervised autoencoders emerge as a more scalable solution, requiring $O(N)$ training samples and no ground truth GED to be optimized on. This allows faster calculation of counterfactual explanations.

We could safely attribute the lower autoencoder performance to the significantly smaller training dataset size; therefore, increasing the number of training samples N could lead to advanced performance. Despite this case still being computationally affordable, it is not applicable in low-resource scenarios where a larger number of high-quality graphs cannot be guaranteed, or where graphs need to be constructed manually. Overall, it depends on the application and the availability of data to decide if a larger number of graphs can be employed in the more lightweight unsupervised setting, or if data acts as a major constraint, and therefore supervised approaches are necessitated.

In any case, both supervised and unsupervised approaches are computationally efficient in terms of time and hardware needed. More precisely, training of unsupervised autoencoders on $N=500$ graphs takes less than 2 minutes, while training of supervised GNNs on $\sim N^2/2=70K$ graphs requires ~ 3 hours, with slight variations depending on the density of the input graphs. The training module is the only one that differs between these two approaches, since consequent operations are independent of the model that produced the embedding representations. Therefore, retrieval times (finding the closest counterfactual graph $G_{i_{cc}}$ embedding to the reference graph G_{i_r} embedding using cosine similarity), inference times (producing embeddings from the already trained models), and edit path computation times (calculating GED between the two counterfactual graphs G_{i_r} , $G_{i_{cc}}$) are the same.

Training of both supervised and unsupervised GNNs is feasible on a single GPU available in online platforms (such as Kaggle or Google Colab), while retrieval and inference operations only require a CPU. Therefore, executing and reproducing the reported results is feasible for any user.

Qualitative Results

A qualitative analysis is crucial, as our counterfactual application lies in the visual domain. Even though some models may present similar ranking metrics, we cannot conclude about their quality according to visual perception from merely observing numerical values. This fact is essential in the case of graphs, as either structural or semantic-based cues may be more influential.

In Figure 3, we showcase qualitative counterfactual results employing kernels, as well as both supervised and unsupervised GNNs. The instances presented were acquired from the top-performing models in each scenario, specifically the supervised GCN, unsupervised ARVGA-GIN, and

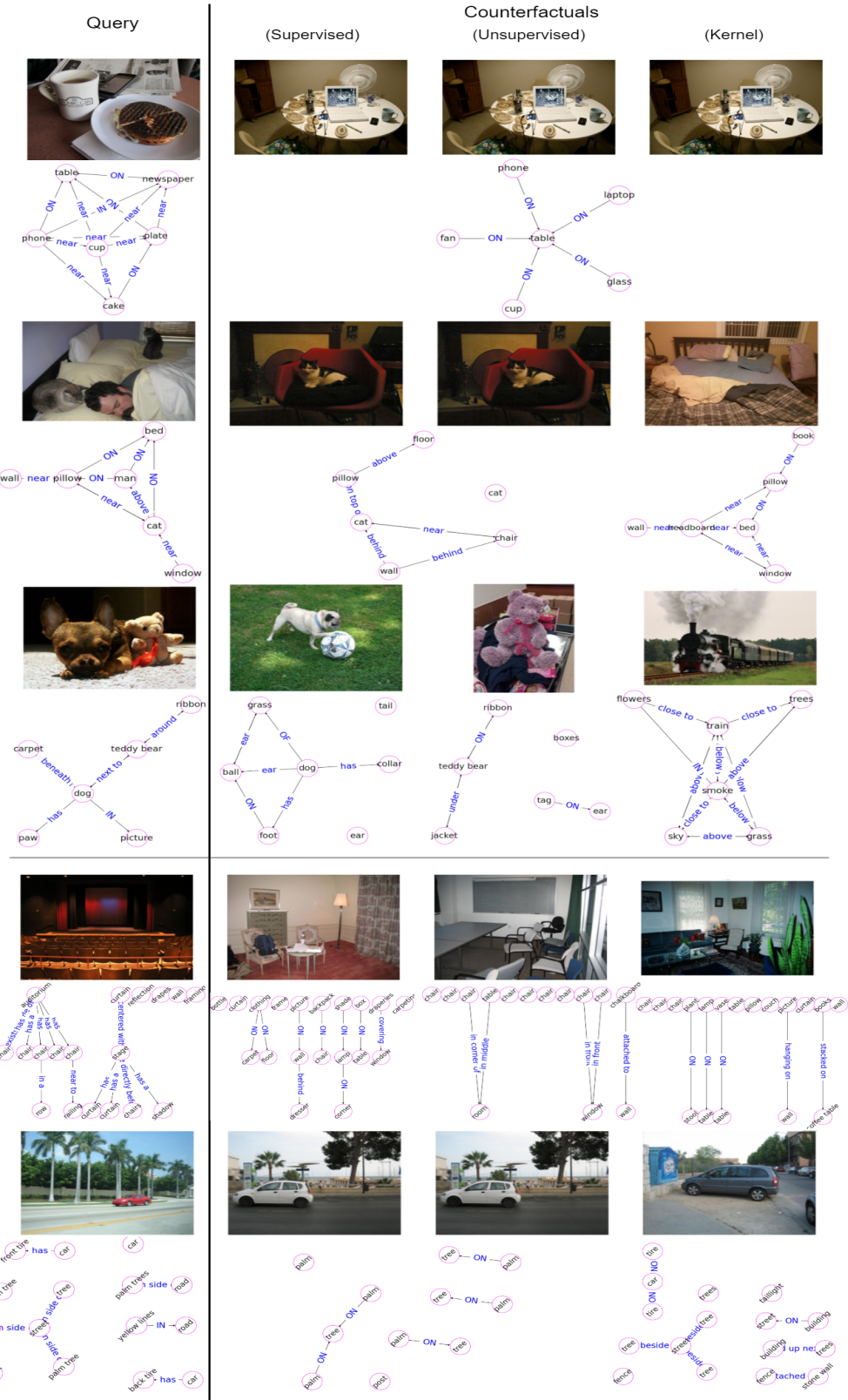


Figure 3: Qualitative examples for counterfactuals retrieved by the best supervised GNN, unsupervised GNN and kernel for each VG subset, VG-DENSE (top 3 examples) and VG-RANDOM (bottom 2 examples).

WL-kernel. Note that counterfactual classes do not need to align between models.

In the case of VG-DENSE, multiple instances exhibit concordance among models, owing to its dense interconnections and the inherent ability of all models to recognize matching structures. The initial row demonstrates unanimous agreement, as the obtained scene graph essentially forms a subgraph of the query. A human could also agree on the semantic closeness between counterfactual instances: The query image corresponds to a "kitchen" table, where a person can have breakfast, while drinking coffee and reading their newspaper. The retrieved instances denote a "workstation" table, where a person can work on their laptop while also drinking a cup of coffee. Semantics such as "table", "cup", "phone" are preserved between counterfactual instances, while the kitchen-related "cake" and "newspaper" semantics should be edited to allow workstation-related semantics, such as "laptop".

Moving to the second row, GNN methods align due to their adeptness in integrating both structural and semantic information. Despite the kernel-retrieved result having a more similar structure, GNN methods successfully discern and retrieve an image featuring a cat on furniture, surpassing a mere depiction of a bed: the knowledge-based semantics allow the information of the WordNet hierarchy *bed-isA-furniture* and *chair-isA-furniture* to drive counterfactual retrieval. In terms of human perception, counterfactuals depicting a "bedroom" (query) and a "living room" instance (GNN-based retrievals) respect the change of class label ("bedroom"→"living room") with minimally altering semantics ("pillow" and "cat" semantics are preserved), allowing effortless high-level interpretability.

Conversely, in the third row with a widespread disagreement, the merits of the supervised GNN network become evident. The unsupervised GAE captures an image resembling the query with a teddy bear wearing a bow but overlooks the presence of a dog, leading to decreased preservation of semantics. In contrast, the supervised GNN, having more accurately approximated GED, retrieves an image centered on a dog and a toy, while altering the class from "living room" to "garden". Although the toy may differ, the semantic proximity of the pug image is notable. Once again, hierarchical knowledge allows this abstraction (*teddy bear-isA-toy* and *ball-isA-toy*, offering high-level interpretability of suggested counterfactuals. Interestingly, the kernel fails and retrieves an image of a train, emphasizing that a sole focus on structure is insufficient. While the kernel aligns with the star shape of the query's scene graph, the interconnected objects differ entirely, and the depicted scenes are totally unrelated.

Concerning VG-RANDOM, assessing retrieved results proves challenging due to the dissimilar nature of the sparser underlying graphs. In the fourth row, the supervised GCN retrieves a structurally closer scene graph, despite visual similarities in GNN-based counterfactuals. It becomes harder even for humans to evaluate the proximity of such counterfactuals, since all instances contain "chair" and "curtain" concepts, but no other discriminative structure or detail.

In the final row, GNN models reach consensus, successfully retrieving an image featuring palm trees, a character-

istic the kernel fails to achieve despite the retrieval of very closely aligned graphs. The closeness of VG-RANDOM results highlights that our counterfactual framework requires rich interconnections to perform in a meaningful manner. At the same time, interconnections are indeed meaningful to humans, as proven by VG-DENSE examples, where evaluation of counterfactuals was easier and more interpretable, in contrast to VG-RANDOM retrievals. This observation aligns with the question regarding the relatedness between expressive scene graphs and human intuition, since concept interconnections may be highly informative (as in the case of the running example of Figure 1). To our favor, data pre-processing can eliminate sparser graphs from our analysis, enabling more informative explanations.

Notably, none of the retrieved instances are misled by purely visual characteristics, such as color, contrast or brightness of images. This is because our graph-based algorithms naturally disregard any such characteristics, as they are not integrated into scene graphs, allowing a more human-related interpretation. This fact becomes evident if we think about e.g. a kitchen instance, such as the one in the first row. Even if we convert this image to grayscale or if we increase/decrease brightness, it still remains an image of a kitchen, depicting the same objects. A human could effortlessly insist that the new image still depicts the same image under all these conversions, concluding that graph machine learning models, and especially GNNs are capable to fully align with human perception.

Conclusion

In this work, we introduce a novel framework that employs Graph Machine Learning algorithms that optimize the search of conceptual edits to provide counterfactual explanations of images. Scene graphs are leveraged as a means for conceptual representation of a given image, highlighting the importance of interconnections, which was missing from previous conceptual counterfactual frameworks. Under this abstraction, searching for counterfactual scenes reduces to a graph matching problem, while knowledge-based edit costs suggest the conceptually minimum changes needed to be made on a given graph to change its classification label. A variety of graph based algorithms, including graph kernels, supervised and unsupervised graph neural networks demonstrate the merits of our proposed framework, which significantly accelerates the graph matching procedure without exhaustively calculating graph edit distance for all graph pairs of the dataset. Quantitative and qualitative analysis showcases the different criteria that influence the retrieval of counterfactual instances from varying graph algorithms, and the importance of well-defined and informative semantics towards human-interpretable explanations. Overall, our conceptual counterfactual framework provides insightful information on what needs to be changed conceptually to transit to another classification label, providing optimality guarantees from knowledge bases and computational efficiency from utilizing lightweight graph models.

References

- Abid, A.; Yuksekgonul, M.; and Zou, J. 2022. Meaningfully Debugging Model Mistakes using Conceptual Counterfactual Explanations. *arXiv:2106.12723*.
- Akula, A.; Wang, S.; and Zhu, S. 2020. CoCoX: Generating Conceptual and Counterfactual Explanations via Fault-Lines. *Proceedings of the AAAI Conference on Artificial Intelligence*, 34: 2594–2601.
- Augustin, M.; Boreiko, V.; Croce, F.; and Hein, M. 2022. Diffusion Visual Counterfactual Explanations. *arXiv:2210.11841*.
- Bird, S.; Klein, E.; and Loper, E. 2009. *Natural Language Processing with Python: Analyzing Text with the Natural Language Toolkit*. Beijing: O'Reilly. ISBN 978-0-596-51649-9.
- Borgwardt, K.; and Kriegel, H. 2005. Shortest-path kernels on graphs. In *Fifth IEEE International Conference on Data Mining (ICDM'05)*, 8 pp.–.
- Browne, K.; and Swift, B. 2020. Semantics and explanation: why counterfactual explanations produce adversarial examples in deep neural networks. *arXiv:2012.10076*.
- Chang, C.-H.; Creager, E.; Goldenberg, A.; and Duvenaud, D. 2019. Explaining Image Classifiers by Counterfactual Generation. *arXiv:1807.08024*.
- Chang, X.; Ren, P.; Xu, P.; Li, Z.; Chen, X.; and Hauptmann, A. 2023. A Comprehensive Survey of Scene Graphs: Generation and Application. *IEEE Transactions on Pattern Analysis and Machine Intelligence*, 45(1): 1–26.
- Dervakos, E.; Thomas, K.; Filandrianos, G.; and Stamou, G. 2023. Choose your Data Wisely: A Framework for Semantic Counterfactuals. *arXiv:2305.17667*.
- Farid, K.; Schrodi, S.; Argus, M.; and Brox, T. 2023. Latent Diffusion Counterfactual Explanations. *ArXiv*, abs/2310.06668.
- Fey, M.; and Lenssen, J. E. 2019. Fast Graph Representation Learning with PyTorch Geometric. In *ICLR Workshop on Representation Learning on Graphs and Manifolds*.
- Filandrianos, G.; Thomas, K.; Dervakos, E.; and Stamou, G. 2022. Conceptual Edits as Counterfactual Explanations. In *Proceedings of the AAAI 2022 Spring Symposium on Machine Learning and Knowledge Engineering for Hybrid Intelligence (AAAI-MAKE 2022)*, Stanford University, Palo Alto, California, USA.
- Gärtner, T.; Flach, P.; and Wrobel, S. 2003. On Graph Kernels: Hardness Results and Efficient Alternatives. In Schölkopf, B.; and Warmuth, M. K., eds., *Learning Theory and Kernel Machines*, 129–143. Berlin, Heidelberg: Springer Berlin Heidelberg. ISBN 978-3-540-45167-9.
- Goodfellow, I.; Pouget-Abadie, J.; Mirza, M.; Xu, B.; Warde-Farley, D.; Ozair, S.; Courville, A.; and Bengio, Y. 2014. Generative Adversarial Nets. In Ghahramani, Z.; Welling, M.; Cortes, C.; Lawrence, N.; and Weinberger, K., eds., *Advances in Neural Information Processing Systems*, volume 27. Curran Associates, Inc.
- Goyal, Y.; Wu, Z.; Ernst, J.; Batra, D.; Parikh, D.; and Lee, S. 2019. Counterfactual Visual Explanations. *arXiv:1904.07451*.
- Hasibi, R.; and Michoel, T. 2020. A Graph Feature Auto-Encoder for the Prediction of Unobserved Node Features on Biological Networks. *arXiv:2005.03961*.
- Hendricks, L. A.; Hu, R.; Darrell, T.; and Akata, Z. 2018. Grounding Visual Explanations. *arXiv:1807.09685*.
- Hido, S.; and Kashima, H. 2009. A Linear-Time Graph Kernel. In *2009 Ninth IEEE International Conference on Data Mining*, 179–188.
- Jonker, R.; and Volgenant, A. 1987. A shortest augmenting path algorithm for dense and sparse linear assignment problems. *Computing*, 38(4): 325–340.
- Kipf, T. N.; and Welling, M. 2016a. Semi-supervised classification with graph convolutional networks. *arXiv preprint arXiv:1609.02907*.
- Kipf, T. N.; and Welling, M. 2016b. Variational Graph Auto-Encoders. *arXiv:1611.07308*.
- Kondor, R. 2002. Diffusion kernels on graphs and other discrete structures. In *International Conference on Machine Learning*.
- Krishna, R.; Zhu, Y.; Groth, O.; Johnson, J.; Hata, K.; Kravitz, J.; Chen, S.; Kalantidis, Y.; Li, L.-J.; Shamma, D. A.; et al. 2017. Visual genome: Connecting language and vision using crowdsourced dense image annotations. *International journal of computer vision*, 123(1): 32–73.
- Li, Y.; Gu, C.; Dullien, T.; Vinyals, O.; and Kohli, P. 2019. Graph Matching Networks for Learning the Similarity of Graph Structured Objects. *arXiv:1904.12787*.
- Loshchilov, I.; and Hutter, F. 2019. Decoupled Weight Decay Regularization. *arXiv:1711.05101*.
- Lymperaiou, M.; Filandrianos, G.; Thomas, K.; and Stamou, G. 2023. Counterfactual Edits for Generative Evaluation. *arXiv:2303.01555*.
- Manning, C. D.; Raghavan, P.; and Schütze, H. 2008. *Introduction to Information Retrieval*. USA: Cambridge University Press. ISBN 0521865719.
- Miller, G. A. 1995. WordNet: a lexical database for English. *Communications of the ACM*, 38(11): 39–41.
- OpenAI. 2023a. ChatGPT: Conversational Language Model. <https://www.openai.com/research/chatgpt>.
- OpenAI. 2023b. GPT-4 Technical Report. *ArXiv*, abs/2303.08774.
- Pan, S.; Hu, R.; Long, G.; Jiang, J.; Yao, L.; and Zhang, C. 2019. Adversarially Regularized Graph Autoencoder for Graph Embedding. *arXiv:1802.04407*.
- Poyiadzi, R.; Sokol, K.; Santos-Rodriguez, R.; De Bie, T.; and Flach, P. 2020. FACE: Feasible and Actionable Counterfactual Explanations. In *Proceedings of the AAAI/ACM Conference on AI, Ethics, and Society*, AIES '20. ACM.
- Pržulj, N. 2007. Biological network comparison using graphlet degree distribution. *Bioinformatics*, 23(2): e177–e183.

- Rudin, C. 2019. Stop Explaining Black Box Machine Learning Models for High Stakes Decisions and Use Interpretable Models Instead. *arXiv:1811.10154*.
- Sanfeliu, A.; and Fu, K.-S. 1983. A distance measure between attributed relational graphs for pattern recognition. *IEEE Transactions on Systems, Man, and Cybernetics*, SMC-13(3): 353–362.
- Shervashidze, N.; Schweitzer, P.; van Leeuwen, E. J.; Mehlhorn, K.; and Borgwardt, K. M. 2011. Weisfeiler-Lehman Graph Kernels. *Journal of Machine Learning Research*, 12(77): 2539–2561.
- Siglidis, G.; Nikolentzos, G.; Limnios, S.; Giatsidis, C.; Skianis, K.; and Vazirgiannis, M. 2020. GraKeL: A Graph Kernel Library in Python. *arXiv:1806.02193*.
- Vandenhende, S.; Mahajan, D.; Radenovic, F.; and Ghadiyaram, D. 2022. Making Heads or Tails: Towards Semantically Consistent Visual Counterfactuals. *arXiv preprint arXiv:2203.12892*.
- Veličković, P.; Cucurull, G.; Casanova, A.; Romero, A.; Lio, P.; and Bengio, Y. 2017. Graph attention networks. *arXiv preprint arXiv:1710.10903*.
- Wachter, S.; Mittelstadt, B.; and Russell, C. 2018. Counterfactual Explanations without Opening the Black Box: Automated Decisions and the GDPR. *arXiv:1711.00399*.
- Xu, K.; Hu, W.; Leskovec, J.; and Jegelka, S. 2018. How powerful are graph neural networks? *arXiv preprint arXiv:1810.00826*.
- Zhao, W.; Oyama, S.; and Kurihara, M. 2020. Generating Natural Counterfactual Visual Explanations. In *International Joint Conference on Artificial Intelligence*.
- Zhou, B.; Lapedriza, A.; Khosla, A.; Oliva, A.; and Torralba, A. 2017. Places: A 10 million Image Database for Scene Recognition. *IEEE Transactions on Pattern Analysis and Machine Intelligence*.